TBR1 directly represses *Fezf2* to control the laminar origin and development of the corticospinal tract

Wenqi Han[1], Kenneth Y. Kwan[1], Sungbo Shim[1], Mandy M. S. Lam, Yurae Shin, Xuming Xu, Ying Zhu, Mingfeng Li, and Nenad Šestan[2]

Department of Neurobiology, Kavli Institute of Neuroscience, Yale University School of Medicine, New Haven, CT 06510

Edited by Edward G. Jones, University of California, Davis, CA, and approved January 7, 2011 (received for review November 9, 2010)

The corticospinal (CS) tract is involved in controlling discrete voluntary skilled movements in mammals. The CS tract arises exclusively from layer (L) 5 projection neurons of the cerebral cortex, and its formation requires L5 activity of *Fezf2* (*Fezl*, *Zfp312*). How this L5-specific pattern of *Fezf2* expression and CS axonal connectivity is established with such remarkable fidelity had remained elusive. Here we show that the transcription factor TBR1 directly binds the *Fezf2* locus and represses its activity in L6 corticothalamic projection neurons to restrict the origin of the CS tract to L5. In *Tbr1* null mutants, CS axons ectopically originate from L6 neurons in a *Fezf2*-dependent manner. Consistently, misexpression of *Tbr1* in L5 CS neurons suppresses *Fezf2* expression and effectively abolishes the CS tract. Taken together, our findings show that TBR1 is a direct transcriptional repressor of *Fezf2* and a negative regulator of CS tract formation that restricts the laminar origin of CS axons specifically to L5.

neocortex | pyramidal neuron | axon guidance | transcriptional repression

Spatial specificity of axonal connections is one of the most important prerequisites for normal development (1–3). In mammals, this is especially crucial for axons of the corticospinal (CS) system (4–7). Development of the CS tract is an intricate process that involves the molecular specification of CS neurons and axon pathfinding. All long-range subcortical axons projecting to the brainstem and spinal cord, including those that form the CS tract, originate exclusively from layer (L) 5 projection (pyramidal) neurons of the cerebral cortex (8–11). Projection neurons in other cortical layers give rise to axons that project within the cortex (L2–4) or to the thalamus (L6). How this highly conserved laminar pattern of projections is formed with such perfect accuracy remains elusive.

Previous work revealed that the transcription factor FEZF2 (FEZL, ZFP312) is highly enriched in L5 CS neurons and is critical to the development of the CS tract (12–14). Inactivation of *Fezf2* disrupts formation of the CS tract (12–14), whereas misexpression of *Fezf2* in upper layer projection neurons induces ectopic subcortical projections (13). These findings indicate that *Fezf2* transcription is tightly regulated during development, and that the integrity of normal *Fezf2* expression is critical to proper development of the CS tract. Interestingly, *Fezf2* is transiently expressed in L6 neurons during early embryonic development, where its transcription is directly repressed by SOX5, thereby establishing a high-in-L5, low-in-L6 postnatal pattern (15, 16). Paradoxically, in *Sox5* null mutants, the number of axon projections reaching the brainstem and spinal cord is severely reduced despite increased cortical *Fezf2* expression (15). This suggests that *Sox5* is required for the formation of these connections independent of its regulation of *Fezf2*. Furthermore, SOX5 is normally expressed in L5 *Fezf2*-expressing CS neurons (15). Therefore, the down-regulation of *Fezf2* in L6 neurons, and hence the establishment of *Fezf2's* L5 pattern, likely requires additional molecules. Recently, Bedogni et al. (17) showed that TBR1 exerts positive and negative control over a number of genetic markers of regional (areal) and laminar identity. Notably, *Tbr1* null mutants exhibit an increase in *Fezf2* expression concomitant with a decrease in *Sox5* expression. Those findings, along with the observation that *Tbr1* null mutants exhibit axon projection defects with some similarities to those of the *Sox5* null phenotype (17, 18), led to the hypothesis that *Tbr1* regulates *Fezf2* expression indirectly via *Sox5*.

In the present study, we tested the alternative hypothesis that *Tbr1* directly represses *Fezf2* transcription and thereby controls the laminar origin and development of the CS tract. We found that TBR1 binds directly to a conserved regulatory element near the *Fezf2* gene and selectively represses its activity in L6 corticothalamic projection neurons. Moreover, in *Tbr1* null mutants, CS axons originate ectopically from L6 neurons in a *Fezf2*-dependent manner. Consistent with this, TBR1 was absent from *Fezf2*-expressing L5 CS tract neurons during development, and the forced expression of *Tbr1* in these neurons suppressed *Fezf2* and blocked CS tract formation. Taken together, our findings show that TBR1 is a direct transcriptional repressor of *Fezf2* that blocks the formation of the CS tract from L6, thereby restricting the origin of CS axons specifically to L5.

Results

TBR1 Binds Directly to a Consensus Site Near *Fezf2*. Using microarrays to analyze changes in the *Tbr1* null cortical transcriptome, Bedogni et al. (17) found a significant increase in *Fezf2* expression, and suggested that this up-regulation is a result of decreased *Sox5* expression. Our independent analyses using mRNA-Seq (Fig. 1*A*), quantitative RT-PCR (qRT-PCR; Fig. 2*A*), and in situ hybridization (ISH; Fig. 2*B*) confirmed a significant up-regulation of *Fezf2* in *Tbr1*$^{-/-}$ neocortex. However, analysis by immunostaining and immunoblotting revealed that SOX5 protein levels were relatively unaltered in late embryonic and neonatal *Tbr1*$^{-/-}$ cortex (Fig. S1). This led us to the hypothesis that TBR1 regulates *Fezf2* transcription via direct binding to regulatory sequences near *Fezf2*. To identify genome-wide TBR1 binding sites in an unbiased and hypothesis-independent manner, we analyzed TBR1-immunoprecipitated chromatin using deep sequencing (ChIP-Seq; Fig. 1*B*). We tested several available anti-TBR1 antibodies and found that none was suitable for immunoprecipitating chromatin of sufficient quality for ChIP-Seq. Thus, we generated a V5-TBR1 fusion construct and expressed it in N2A cells. V5-TBR1 was immunoprecipitated using an anti-V5 antibody. DNA-Seq was performed on the Illumina GAIIx platform, and data were analyzed as described in *SI Materials and Methods*. A total of 34.5 million reads of 36 bp were generated for V5-precipitated chromatin and 37 million reads were generated for control input DNA,

Author contributions: W.H., K.Y.K., and N.Š. designed research; W.H., K.Y.K., S.S., M.M.S.L., and Y.S. performed research; W.H., K.Y.K., X.X., Y.Z., M.L., and N.Š. analyzed data; and W.H., K.Y.K., and N.Š. wrote the paper.

The authors declare no conflict of interest.

This article is a PNAS Direct Submission.

Freely available online through the PNAS open access option.

[1]W.H., K.Y.K., and S.S. contributed equally to this work.

[2]To whom correspondence should be addressed. E-mail: nenad.sestan@yale.edu.

This article contains supporting information online at www.pnas.org/lookup/suppl/doi:10.1073/pnas.1016723108/-/DCSupplemental.

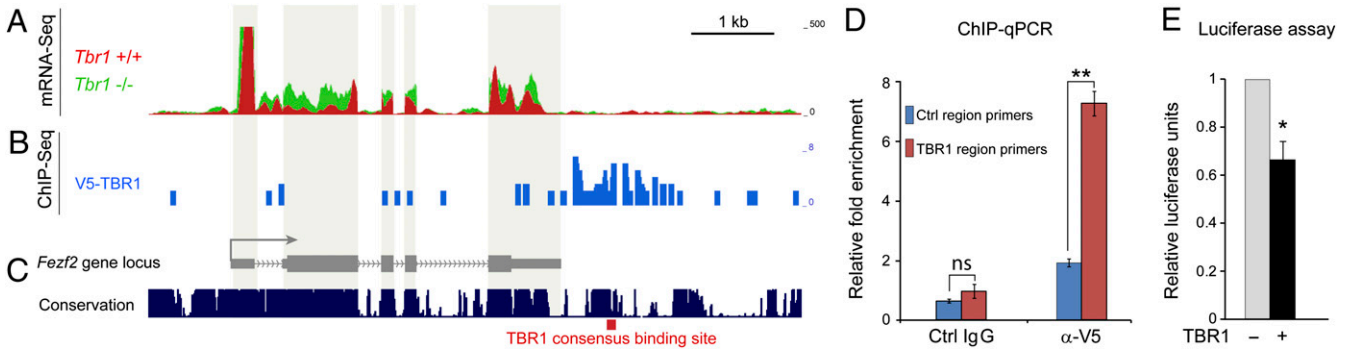

Fig. 1. TBR1 regulates *Fezf2* transcription via direct binding and repression of regulatory elements near *Fezf2*. (*A*) RNA-Seq of mRNA extracted from neocortices of P0 *Tbr1*$^{-/-}$ and *Tbr1*$^{+/+}$ littermates (n = 2 per genotype). Significantly more RNA-Seq reads mapped to *Fezf2* exons (gray) in *Tbr1*$^{-/-}$ (green; 727 reads) than in *Tbr1*$^{+/+}$ (red, 496 reads; adjusted P value = 1.49E-9). (*B*) N2a cells were transfected with V5-TBR1, and chromatin was immunoprecipated using an anti-V5 antibody. ChIP-Seq revealed enrichment of mapped reads (blue) compared with input DNA in a region 4.5 kb downstream of the *Fezf2* TSS. (*C*) Schematic of the mouse *Fezf2* locus (gray) and mammalian conservation (dark blue) showing the location of the TBR1 consensus binding site (red) defined by ChIP-Seq (detailed in Fig. S2). (*D*) ChIP–qRT-PCR assays in neurons cultured from E13.5 neocortex transfected with V5-TBR1. DNA precipitated with control rabbit IgG or anti-V5 antibody was analyzed by qRT-PCR using primers flanking the TBR1 binding site and control primers. The TBR1 site was significantly enriched in V5-precipitated DNA. (*E*) N2A cells were transfected with luciferase plasmids containing the TBR1 binding site. Luciferase assay showed that cotransfection of CAG-*Tbr1*, but not of empty CAG, repressed the activity of this element. *P < 0.02; **P < 0.005 by unpaired two-tailed t test. ns, not significant (P > 0.05).

of which 82.9% and 85.1%, respectively, uniquely mapped to the genome. Of immunoenriched regions with a false discovery rate cutoff of 0.02, approximately 62% were mapped within gene loci, and an additional 28% were mapped within 50 kb upstream of transcription start sites (TSSs) or 50 kb downstream of the polyadenylation signal.

To identify putative TBR1 consensus binding sequences with potential relevance to TBR1 transcriptional activity in the neocortex, we cross-analyzed our mRNA-Seq and ChIP-Seq data. We selected the loci of significantly differentially expressed genes based on mRNA-Seq data to which a significant enrichment of TBR1 ChIP-Seq reads mapped proximally. Analysis of these 181 loci (detailed in *SI Material and Methods*) revealed a binding sequence motif (Fig. S2) with similarities to the T element in *Xenopus* (19, 20). Importantly, an enrichment of TBR1 ChIP-Seq reads compared with input DNA was mapped to a highly conserved region ~4.5 kbp downstream of the *Fezf2* TSS. This region contained a core consensus binding site conserved across placental mammalian species (Fig. 1*C* and Fig. S2*C*). To confirm this binding in the neocortex, we performed ChIP using cultured embryonic day (E) 13.5 neocortical neurons transfected with V5-TBR1. Analysis of ChIPed DNA by qRT-PCR revealed a significant enrichment of this binding site in DNA precipitated by V5 antibody compared with control IgG (a 6.65 ± 0.37-fold increase; P = 0.00128) (Fig. 1*D*), confirming that TBR1 binds this region in neocortical neurons. To assess whether this binding affects transcription, we cloned the binding site downstream of the luciferase reporter gene and assayed transfected N2a cells. Forced expression of *Tbr1* moderately but significantly repressed the activity of this binding site (a decrease of 31.9% ± 8.6%; P = 0.0105) (Fig. 1*E*). Collectively, these findings suggest that TBR1 negatively regulates *Fezf2* transcription through direct binding to a conserved consensus element.

L6 Neurons Aberrantly Retain High *Fezf2* Expression in *Tbr1* Null Mutants. The global increase in *Fezf2* expression in the early postnatal *Tbr1*$^{-/-}$ neocortex found in the present study and a previous study (17) could result from either up-regulation of *Fezf2* in neurons that normally express *Fezf2* or ectopic expression of *Fezf2* in neurons that do not normally express *Fezf2*. Consistent with the latter possibility, analysis of TBR1 expression during cortical development revealed that TBR1 and *Fezf2* established complementary laminar expression patterns during late embryogenesis (Fig. S3*A*). To directly assess how TBR1 alters *Fezf2* expression at the level of resolution of individual neurons, we bred *Tbr1*$^{+/-}$ mice with *Fezf2-Gfp* transgenic mice. In the postnatal day (P) 0 *Tbr1*$^{-/-}$ neocortex, the number of neurons highly expressing *Fezf2-Gfp*, which did not migrate normally (18), increased significantly from 21.8% in *Tbr1*$^{+/+}$ to 33.3% in *Tbr1*$^{-/-}$ (P = 0.0058) (Fig. 2*C*). This significant increase in the total number of *Fezf2-Gfp*–expressing neurons in *Tbr1*$^{-/-}$ neocortex reflects an aberrant induction of high *Fezf2* expression in neurons that do not normally express *Fezf2*.

Because TBR1 is specifically expressed in L6 neurons at P0, we examined whether L6 neurons aberrantly turned on high *Fezf2* expression in the *Tbr1*$^{-/-}$ neocortex. We used two stringent criteria to conservatively define L6 neurons in the *Tbr1*$^{-/-}$ neocortex, in which the demarcation of distinct layers is complicated by migration defects (ref. 18 and Fig. S4). First, we chose ZFPM2 (FOG2) to molecularly define L6 neurons, because it is a reliable marker of L6 corticothalamic neurons in the early postnatal neocortex (ref. 15 and Fig. S5) and, more importantly, because its expression level is unchanged in *Tbr1*$^{-/-}$ neocortex (Fig. S6, mRNA-Seq; P = 0.642 and ref. 17). Second, we used a stringent birth-dating strategy to distinguish L6 neurons from L5 neurons. In the sequential generation of cortical neurons, the same progenitor cells that give rise to L6 neurons subsequently give rise to L5 neurons. Therefore, positive thymidine analog incorporation of L6 neurons will inevitably label a large number of L5 neurons. To circumvent this, we used exclusion of the thymidine analog CldU to distinguish L6 and L5 neurons. CldU was administered to timed-pregnant *Tbr1*$^{+/-}$ females daily starting at E12.5, when the first L5 neurons are born, and ending at E14.5, when the last L5 neurons are generated. Using this narrow definition of L6 neurons (ZFPM2^{+}, CldU^{-}), we observed a significant increase in the number of L6 neurons expressing *Fezf2-Gfp* (18.5% in *Tbr1*$^{+/+}$ and 85.9% in *Tbr1*$^{-/-}$; P = 0.000031) (Fig. 2*D*). Thus, in the absence of *Tbr1*, neurons born at the correct time and with the molecular properties of L6 neurons ectopically expressed high levels of *Fezf2*.

Ectopic L6 Projections to the Brainstem Are Revealed by Retrograde Tracing in *Tbr1* Null Mutants. Subcortical axon defects have been reported in *Tbr1*$^{-/-}$ brains (18). Long-range subcerebral axons and the layer-specific pattern of cortical connectivity have not been specifically examined, however. To test whether aberrantly high expression of *Fezf2* in L6 neurons leads to the formation of ectopic projections to the brainstem, we bred *Tbr1*$^{+/-}$ mice with *Golli-Gfp* transgenic mice, which express GFP predominantly in L6 and SP neurons and their axons (21), and with *Fezf2-Gfp*

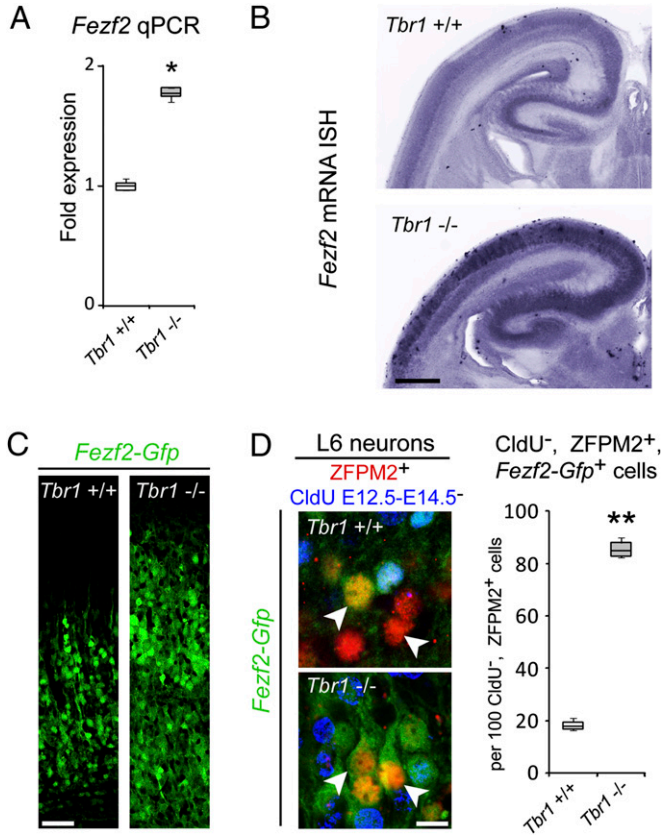

Fig. 2. High *Fezf2* expression is aberrantly retained in neonatal L6 neurons in $Tbr1^{-/-}$ neocortex. (*A*) qRT-PCR of P0 neocortical mRNA. Normalized to *Gapdh*, *Fezf2* expression levels increased by 1.77 ± 0.08-fold in $Tbr1^{-/-}$ compared with $Tbr1^{+/+}$. (*B*) *Fezf2* ISH of P0 brains showed increased *Fezf2* expression in $Tbr1^{-/-}$ neocortex. (Scale bar: 500 μm.) (*C*) P0 neocortices of $Tbr1^{+/+}$ and $Tbr1^{-/-}$ littermates transgenic for *Fezf2-Gfp*. *Fezf2-Gfp*–expressing neurons were dispersed in the $Tbr1^{-/-}$, consistent with previously reported defects in neuronal migration (18). The proportion of neurons expressing *Fezf2-Gfp* significantly increased from 21.8% in the $Tbr1^{+/+}$ to 33.3% in the $Tbr1^{-/-}$ (1.53 ± 0.27-fold). (Scale bar: 50 μm.) (*D*) L6 neurons (arrowhead) were stringently defined by expression of the L6 corticothalamic neuron marker ZFPM2 (red) and a lack of incorporation of CldU (blue), multiple doses of which were injected daily from E12.5 to E14.5, when L5 neurons were generated. The number of L6 neurons expressing *Fezf2-Gfp* increased significantly from 18.5% in the $Tbr1^{+/+}$ to 85.9% in the $Tbr1^{-/-}$ (4.64 ± 0.20-fold). (Scale bar: 10 μm.) $*P < 0.01$; $**P < 0.00005$ by unpaired two-tailed *t* test.

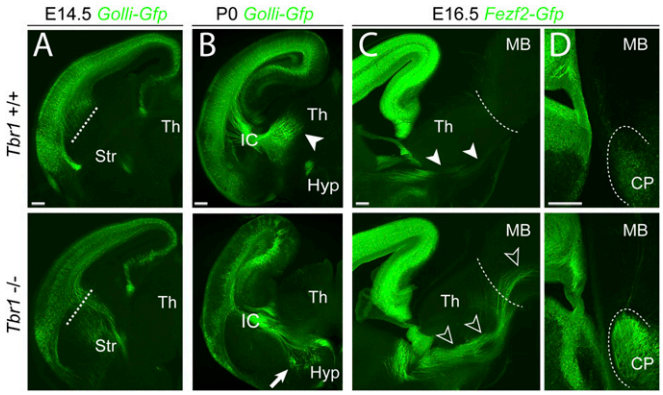

Fig. 3. Premature overgrowth and superabundance of subcortical axons in the brainstem of $Tbr1^{-/-}$ mice. (*A*) In E14.5 $Tbr1^{+/+}$, *Golli-Gfp*$^+$ axons originating mainly from L6 neurons extended to the upper portion of the striatum (Str; above the dashed line). In $Tbr1^{-/-}$, numerous *Golli-Gfp*$^+$ axons extended to the deeper portion of the striatum (below the dashed line) toward the internal capsule. (*B*) In P0 $Tbr1^{-/-}$, *Golli-Gfp*$^+$ axons were not present in the dorsal thalamus (Th), indicating that the normal corticothalamic tract (solid arrowhead) had not formed. Ectopic axons (arrow) were misdirected toward other subcortical targets, including the hypothalamus (Hyp) and the midbrain. (*C*) In E16.5 $Tbr1^{+/+}$ brain, *Fezf2-Gfp*$^+$ axons (solid arrowheads) did not cross the forebrain/midbrain boundary (dashed line). In $Tbr1^{-/-}$, numerous *Fezf2-Gfp*$^+$ axons (open arrowheads) extended subcerebrally to invade the midbrain (MB). (*D*) In E16.5 $Tbr1^{+/+}$ brain, only a few *Fezf2-Gfp*$^+$ axons innervated the CPs (dashed lines). Dramatically more *Fezf2-Gfp*$^+$ axons entered the CPs in $Tbr1^{-/-}$. (Scale bars: 100 μm.)

transgenic mice. In E14.5 normal embryos, *Golli-Gfp* axons en route to the thalamus entered the upper portion of the striatum, but not the lower portion (Fig. 3*A*). In E14.5 $Tbr1^{-/-}$ brains, *Golli-Gfp* axons exhibited premature overgrowth, ectopically invading the lower portion of the striatum and the primitive internal capsule. At P0, numerous *Golli-Gfp* axons reached the dorsal thalamus in $Tbr1^{+/+}$ (Fig. 3*B*, solid arrowhead). In the P0 $Tbr1^{-/-}$ brains, none of the *Golli-Gfp* axons entered the dorsal thalamus, but many were aberrantly directed toward other subcortical targets, including the hypothalamus (Fig. 3*B*, arrow) and the midbrain. Similarly, exuberant *Fezf-Gfp* axons in E16.5 and P0 $Tbr1^{-/-}$ brains (Fig. 3*C*, open arrowheads and Fig. S7), ectopically innervated the cerebral peduncles (CPs; Fig. 3*D*, broken line) and brainstem, indicating that the prematurely outgrown and misguided L6 axons ectopically expressed high levels of *Fezf2-Gfp*.

Normal L6 projection neurons project axons only as far as the thalamus, never reaching the brainstem (8). Our data are consistent with the intriguing possibility that L6 neurons in the $Tbr1^{-/-}$ aberrantly project axons to the brainstem due to increased *Fezf2* expression. Although the *Golli-Gfp* transgene is a useful marker of L6 neurons, a small number of neurons near the L5/L6 border of the cingulate cortex express *Golli-Gfp* and project axons to the brainstem (15). Therefore, the presence of exuberant *Golli-Gfp* axons in the $Tbr1^{-/-}$ brainstem does not unequivocally indicate that the axons originated from L6 neurons. Thus, we performed retrograde axonal tracing by injecting rhodamine-conjugated latex microspheres (LMS) into the pons of $Tbr1^{+/+}$ and $Tbr1^{-/-}$ newborn mice. Analysis was carried out after 18–24 h of survival to allow for transport of the tracer, a time frame that is limited by the perinatal lethality of the $Tbr1^{-/-}$ (22). In addition to the highly stringent criteria described above for identifying L6 neurons using ZFPM2 immunostaining and exclusion of E12.5–E14.5 CldU incorporation, we further narrowed our definition using *Golli-Gfp*, which is mostly restricted to L6 neurons in the somatosensory cortical areas that we analyzed.

In the $Tbr1^{+/+}$, projection neurons labeled retrogradely from the pons were restricted to L5, and most incorporated CldU and expressed neither *Golli-Gfp* nor ZFPM2 (Fig. 4*B*, open arrowheads). A limited number of labeled neurons were positive for *Golli-Gfp* or lacked CldU, but none expressed ZFPM2. Most importantly, as defined by the highly conservative triple criteria (*Golli-Gfp*$^+$, ZFPM2$^+$, and CldU$^-$), no L6 neurons were labeled by the retrograde tracer in any of the traced $Tbr1^{+/+}$ brains (n = 8). In contrast, defined by the same stringent criteria, a considerable number of L6 neurons in the $Tbr1^{-/-}$ somatosensory cortex were clearly labeled by the retrograde tracer, which encircled neuronal nuclei and entered apical dendrites (Fig. 4*C*, solid arrowheads; n = 4 brains). Similar to reported retrograde tracing from the CPs of the $Tbr1^{-/-}$ (18), retrograde tracing from the pons was absent from the most medial cortical areas. Thus, the somatosensory cortex was consistently used for quantification, which revealed a significant increase in the number of labeled L6 neurons in the $Tbr1^{-/-}$ for each of the three criteria used (*Golli-Gfp*$^+$, P = 0.000009; ZFPM2$^+$, P = 0.000007; CldU$^-$, P = 0.000049) (Fig. 4*D*). Notably, the numbers of retrogradely labeled *Golli-Gfp*$^-$ and LSM$^+$ neurons were unaltered in the $Tbr1^{-/-}$ somato-

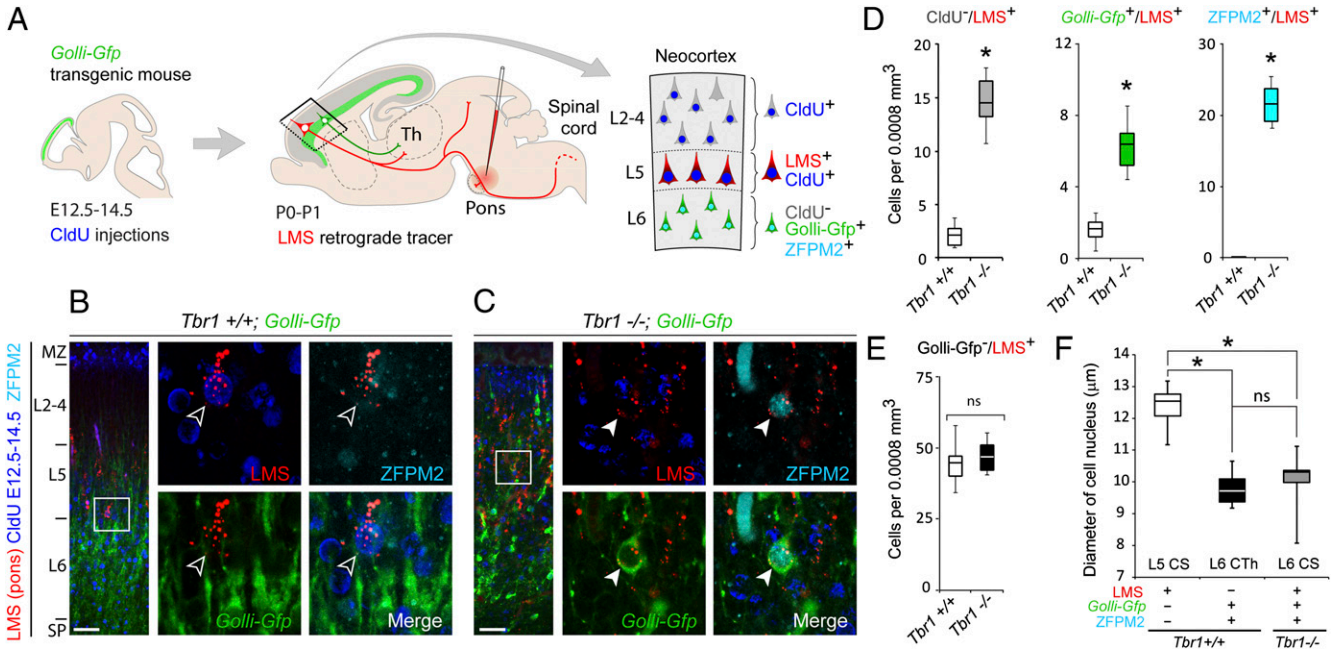

Fig. 4. Stringently defined L6 neurons aberrantly formed subcerebral/CS projections in *Tbr1*$^{-/-}$. (*A*) Schematic of the experimental design. CldU was administered daily between E12.5 and E14.5 to label L5 neurons in timed-pregnant *Tbr1*$^{+/-}$ females transgenic for *Golli-Gfp*. Retrograde tracer (LMS) was injected into the pons of live neonates. L6 neurons were narrowly defined by lack of CldU incorporation and coexpression of *Golli-Gfp* and ZFPM2. (*B* and *C*) Confocal images of the somatosensory cortex were obtained at an optical thickness of 3 μm. (*B*) In *Tbr1*$^{+/+}$, all retrogradely labeled neurons were positioned in L5, and most were *Golli-Gfp*$^{-}$ and ZFPM2^{-} and incorporated CldU (open arrowhead). No neurons meeting our stringent definition of L6 neurons were retrogradely traced in any of the *Tbr1*$^{+/+}$ brains analyzed ($n = 8$). (Scale bar: 50 μm.) (*C*) In *Tbr1*$^{-/-}$, a significant number of L6 neurons meeting our criteria were labeled retrogradely (solid arrowhead; $n = 3$ brains). Ectopic CS projections of these L6 neurons indicate a projectional fate switch. (Scale bar: 50 μm). (*D* and *E*). Quantitative analysis revealed that the number of traced L6 neurons increased significantly in *Tbr1*$^{-/-}$ compared with *Tbr1*$^{+/+}$ for each of the criteria used. However, no difference in the number of traced *Golli-GFP*$^{-}$ L5 neurons was detected. (*F*) Analysis of nucleus diameter. In *Tbr1*$^{+/+}$ neocortex, L5 CS neurons (LMS^{+}) were significantly larger in nuclear diameter compared with L6 corticothalamic neurons (CTh; ZFPM2^{+} and *Golli-Gfp*$^{+}$). In *Tbr1*$^{-/-}$, nuclei of L6 CS neurons (LMS^{+}, ZFPM2^{+}, and *Golli-Gfp*$^{+}$) were indistinguishable in size from *Tbr1*$^{+/+}$ L6 CTh neurons but significantly smaller than *Tbr1*$^{+/+}$ L5 CS neurons. *$P <$ 0.00005 by unpaired two-tailed *t* test. ns, not significant ($P > 0.05$).

sensory cortex (Fig. 4*E*), suggesting that L5 projections to the pons were mostly normal. We also used nuclear size to confirm the identity of the CS neurons projecting to the brainstem and spinal cord. Normal L5 CS neurons (LMS^{+}, ZFPM2^{-}, and *Golli-Gfp*$^{-}$) have larger nuclei compared with L6 corticothalamic neurons (LMS^{-}, ZFPM2^{+}, and *Golli-Gfp*$^{+}$; $P = 2.25\text{E-}17$) (Fig. 4*F*). Analysis of retrogradely traced L6 neurons (LMS^{+}, ZFPM2^{+}, and *Golli-Gfp*$^{+}$) in the *Tbr1*$^{-/-}$ revealed a nuclear diameter indistinguishable from that of normal L6 corticothalamic neurons ($P = 0.168$), but significantly smaller than that of L5 CS neurons ($P = 2.11\text{E-}13$). These data indicate that in the *Tbr1*$^{-/-}$ neocortex, L6 neurons, as stringently defined by marker expression, birthdating, and nuclear size, project axons ectopically to the brainstem instead of to the thalamus and express high levels of *Fezf2*, key features of normal L5 neurons.

Ectopic *Tbr1* Expression in L5 Neurons Effectively Abolishes *Fezf2* Expression and CS Tract Formation. TBR1 is normally excluded from L5 *Fezf2*-expressing CS neurons during embryonic and postnatal development (Fig. S3 *A* and *B*). To investigate whether forced misexpression of *Tbr1* in L5 neurons is able to down-regulate *Fezf2* and suppress CS projections, we performed in utero electroporation at E13.5 to transfect L5 neurons with CAG-*Tbr1* or control empty CAG plasmid DNA, together with CAG-*Rfp* to label neurons generated by electroporated progenitor cells. To analyze *Fezf2* expression in transfected cells, we carried out these experiments in *Fezf2-Gfp* transgenic mice. The vast majority of L5 RFP^{+} neurons electroporated with empty CAG plasmid expressed high levels of *Fezf2-Gfp* (85.3% ± 4.3%) (Fig. 5 *A* and *B*). Remarkably, when *Tbr1* was misexpressed, the number of L5 RFP^{+} neurons expressing high levels of *Fezf2-Gfp* decreased dramatically, to 10.8% ± 4.2% ($P = 0.000003$) (Fig. 5 *A* and *B*). This indicates that *Tbr1* misexpression in L5 neurons is sufficient to suppress *Fezf2* expression.

To investigate whether this repressed *Fezf2* expression functionally affects the axonal projections of L5 CS neurons, we performed in utero electroporation to transfect L5 neurons with CAG-*Tbr1* or empty CAG plasmid DNA, together with CAG-*Gfp*, because the higher solubility of GFP better facilitates the analysis of long-distance CS axons. At E13.5, neurons electroporated with empty CAG plasmid projected corticocortical axons into the corpus callosum (Fig. 5*D*) and projected numerous CS axons into the ventral pons and medullary pyramids (Fig. 5 *E* and *F*). In contrast, GFP^{+} axons originating from L5 neurons misexpressing *Tbr1* were almost completely absent from the pons and pyramids. This disruption of axons was specific to the CS tract, however. *Tbr1*-misexpressing neurons projected abundant GFP^{+} axons into the corpus callosum (Fig. 5*D*). Together, these findings demonstrate that the misexpression of *Tbr1* is sufficient to suppress *Fezf2* expression in L5 neurons and effectively abolish formation of the CS tract.

Induction of Ectopic L6 CS Axons in the *Tbr1* Null Mutants Is Dependent on *Fezf2*. To examine whether the induction of ectopic axons originating from L6 neurons in the *Tbr1*$^{-/-}$ cortex depends on up-regulation of *Fezf2*, we engineered a conditional *Fezf2* allele (Fig. S8 *A* and *B*) for the generation of a cortex-specific *Tbr1; Fezf2* double-null mutant. *Fezf2*$^{flox/flox}$ mice were crossed with *Emx1-Cre* PAC transgenic mice (23) to specifically inactivate *Fezf2* in the cortex (Fig. S8 *A* and *B*). To confirm that our cortex-specific conditional *Fezf2* null mutant was phenotypically similar to germ-line *Fezf2*$^{-/-}$ mice (12, 14), we crossed *Emx1-Cre* PAC;

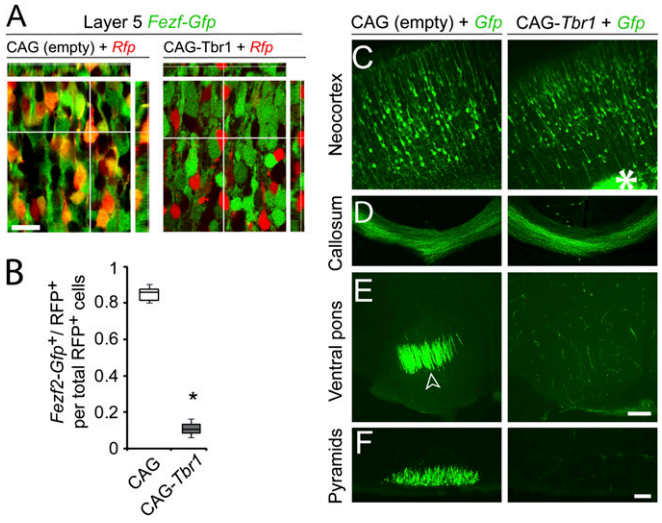

Fig. 5. TBR1 misexpression in L5 neurons abolished *Fezf2* expression and ablated CS axons. (*A* and *B*) CAG-*Tbr1* or empty CAG plasmid DNA was delivered together with CAG-*Rfp* into E13.5 embryos expressing *Fezf2-Gfp* using in utero electroporation. RFP-expressing L5 neurons were examined at P0. Of the L5 neurons electroporated with empty CAG plasmid, 85.3% ± 4.3% expressed *Fezf2-Gfp*. In contrast, only 10.8% ± 4.2% of the *Tbr1*-misexpressing L5 neurons expressed *Fezf2-Gfp*, a significant reduction compared with empty CAG. $P = 0.000003$. (*C–F*) CAG-*Tbr1* or CAG-empty plasmid DNA was coelectroporated with CAG-*Gfp* into WT E13.5 embryos. Brains were collected for analysis at P0. (*C*) The majority of neurons expressing CAG-*Tbr1* migrated normally to settle in all cortical layers, including L5. In all examined brains that overexpressed *Tbr1*, ectopic neuropils and cells were clustered in the white matter (*); however, most axons entered the white matter and innervated the corpus callosum (*D*). Neurons electroporated with empty CAG plasmid projected numerous subcerebral/CS axons into the ventral pons (empty arrowhead) and medullary pyramids. Misexpression of *Tbr1* ablated all CS axons. A few GFP$^+$ axons reached the ventral pons (*E*), but none reached the medullary pyramids (*F*). This indicates that misexpression of TBR1 in L5 neurons substantially down-regulated *Fezf2-Gfp* and blocked formation of the CS tract. (Scale bars: 20 μm in *A*; 200 μm in *C–E*; 50 μm in *F*.)

Fezf2$^{flox/flox}$ mice with CAG-*Cat-Gfp* transgenic mice (24) to reveal the pancortical pattern of axonal connectivity. Similar to germ-line *Fezf2*$^{-/-}$, the CS tract was nearly completely absent from the brainstem (Fig. S8 *C–E*). For analysis of L6 neurons, we bred in the *Golli-Gfp* transgene to generate cortex-specific *Tbr1; Fezf2* double-null mutants (*Tbr1*$^{-/-}$, *Fezf2*$^{fl/fl}$, *Emx1-Cre*, and *Golli-Gfp*). LMS was injected in the pons of *Golli-Gfp* double-null mice and littermate controls at P0. Remarkably, neither L5 nor L6 projection neurons were retrogradely labeled from the pons of the double-null mutants (Fig. 6). Collectively, these data indicate that cortical *Fezf2* activity is required for the formation of ectopic L6 projections to the pons, including the CS system axons in *Tbr1* null mutants, and that *Tbr1* restricts the laminar origin of the CS tract by repressing *Fezf2* in L6 neurons in normal mice.

Discussion

We have shown that TBR1 directly binds a conserved consensus site near the *Fezf2* locus and represses *Fezf2* expression in L6 neocortical projection neurons. In the absence of *Tbr1*, postnatal L6 neurons aberrantly express high levels of *Fezf2* and ectopically project to the brainstem. These ectopic L6 projections to the brainstem, including the CS axons, are *Fezf2*-dependent. Moreover, TBR1 misexpression is sufficient to repress *Fezf2* in L5 neurons and block the formation of the CS tract. These findings (summarized in Fig. S9) demonstrate that TBR1 is a direct transcriptional repressor of *Fezf2* and a negative regulator of the CS tract that restricts the tract's laminar origin specifically to L5.

Our data confirm and extend those of previous studies showing the role of *Tbr1* in the formation of subcortical projections (17, 18). We show here that TBR1 directly represses *Fezf2* and TBR1 overexpression in L5 neurons abolishes CS projections. However, given that L5 CS neurons normally extend collateral axon branches to the dorsal thalamus (25), exogenous expression of TBR1 in these neurons cannot be used to address whether TBR1 is sufficient to confer a corticothalamic projection fate. Notably, the upper-layer neurons, which do not project to the thalamus, normally express TBR1 starting at an early postnatal age. Therefore, it is likely that TBR1, although necessary for normal corticothalamic projections (17, 18), is not sufficient to induce this projection fate.

Using the *Fezf2-Gfp* transgene to reveal the global pattern of corticofugal connections, we found that at P0, the *Tbr1*$^{-/-}$ CS tract is largely of normal size compared with controls (Fig. S7). The additional axons projecting to the brainstem from L6 neurons might be expected to increase the size of this tract in the *Tbr1*$^{-/-}$; however, this increase is likely offset by the role of *Tbr1* in areal patterning (17, 18), in which it is required by neurons in the medial cortex to project subcortical axons. Taken together, these findings indicate that TBR1 is a critical determinant of multiple aspects of cortical development, including neuronal migration, laminar and areal identity, and axonal projection.

The dynamic pattern of *Fezf2* exemplifies how precise temporal and spatial regulation of gene expression has functional consequences in neocortical development and axonal connections. Furthermore, the exclusively postmitotic expression pattern of *Tbr1* (17, 18) indicates that layer-specific molecular and projectional identities are not firmly established during neurogenesis, but undergo postmitotic refinement to establish their mature patterns. This fine-tuning of neuronal identity and connectivity provides a mechanism by which the precise configuration of neural circuits can be modified after neurons integrate into the cortex.

TBR1 is not the only molecule that postmitotically controls the dynamic pattern of *Fezf2* expression. Another transcription factor, SOX5, contributes to this process as well (15, 16). In contrast to the *Tbr1* null mutant, in the *Sox5* null mutants projections to the brainstem are nearly completely abolished (15), indicating that *Sox5* is independently required for the formation of CS tract. Moreover, SOX5 is normally expressed in *Fezf2*-expressing L5 CS neurons (15). These results and our analysis of TBR1 binding sites by ChIP-Seq and ChIP–qRT-PCR are consistent with the hypothesis that TBR1 regulation of *Fezf2* transcription is direct rather than secondary to changes in SOX5 levels, as was previously suggested. Collectively, these data indicate that both SOX5 and TBR1 are required in the regulation of *Fezf2* transcription. Whether the two transcription factors physically interact or cooperate in alternative ways in this role remain unknown, however.

All projections to the brainstem, including the CS system, originate from L5 neurons in all mammalian species examined (4–6). The high degree of conservation indicates that this specific pattern of connectivity is likely critical to the survival and evolutionary success of mammals. It also suggests that the regulatory pathways that establish this pattern are well conserved. Consistent with this, the prenatal neocortical expression patterns of *Fezf2, Tbr1*, and *Sox5* are similar in different mammals, including humans (15, 26, 27). Therefore, TBR1-mediated down-regulation of *Fezf2* in L6 is most likely a conserved mechanism for restricting the laminar origin of the CS tract to L5.

Materials and Methods

Animals. All experiments were carried out in accordance with a protocol approved by Yale University's Committee on Animal Research. *Tbr1* mice were a generous gift from John Rubenstein (22). *Fezf2-Gfp* mice were obtained from GENSAT (28). *Golli-Gfp*, *Emx1-Cre* PAC, and CAG-*Cat-Gfp*

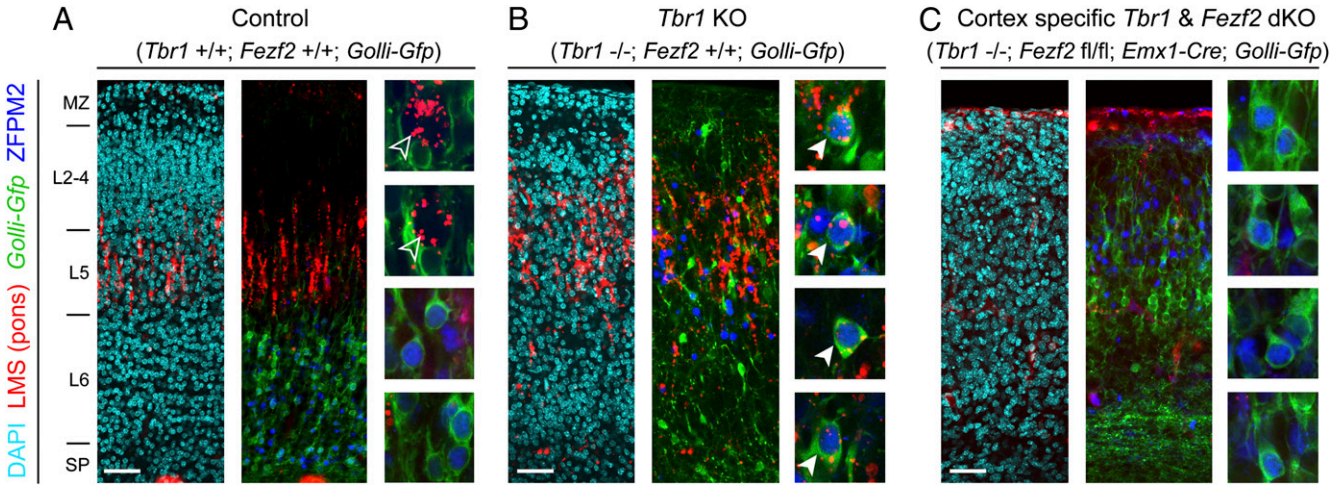

Fig. 6. Aberrant L6 projections to the brainstem in the *Tbr1*$^{-/-}$ require *Fezf2*. Cortex-specific double deletion of *Fezf2* and *Tbr1* was achieved using the *Emx1-Cre* transgene. LMS was injected into the pons of neonatal mice of the indicated genotype. (*A*) In *Tbr1*$^{+/+}$ mice, retrogradely labeled neurons were positioned in L5 and did not express *Golli-Gfp* or ZFPM2 (open arrowheads). (*B*) In *Tbr1*$^{-/-}$ mice, many L6 neurons expressing *Golli-Gfp* and ZFPM2 were retrogradely labeled by LMS (solid arrowheads). (*C*) In *Tbr1*$^{-/-}$;*Fezf2*$^{fl/fl}$;*Emx1-Cre* cortex-specific double mutant, no *Golli-Gfp*$^{+}$ or ZFPM2^{+} L6 neurons were retrogradely labeled. These data indicate a partial rescue of the *Tbr1*$^{-/-}$ phenotype in the absence of cortical *Fezf2* and suggest that the L6 CS projections of *Tbr1*$^{-/-}$ depend on cortical *Fezf2*. (Scale bars: 200 μm.)

mice were generous gifts from Anthony Campagnoni (21), Takuji Iwasato (23) and Melissa Colbert (24), respectively.

Further experimental details can be found in *SI Materials and Methods*.

Note Added in Proof. After the approval of this paper for publication, similar findings by McKenna et al. (29) showed that *Tbr1* and *Fezf2* regulate the alternate corticofugal identities of projection neurons.

ACKNOWLEDGMENTS. We thank A. Louvi, D. McCormick, and members of the N.Š. laboratory for constructive discussions. We especially thank Y. Imamura Kawasawa for preparing sequencing libraries and S. Mane and M. Mahajan for performing sequencing. This work was supported by a grant from the US National Institutes of Health (NS 054273). W.H. and Y.Z. are supported by predoctoral fellowships from the China Scholarship Council, and Y.S. is supported by a predoctoral fellowship from Samsung.

1. Parrish JZ, Emoto K, Kim MD, Jan YN (2007) Mechanisms that regulate establishment, maintenance, and remodeling of dendritic fields. *Annu Rev Neurosci* 30:399–423.
2. Polleux F, Ince-Dunn G, Ghosh A (2007) Transcriptional regulation of vertebrate axon guidance and synapse formation. *Nat Rev Neurosci* 8:331–340.
3. Sanes JR, Yamagata M (2009) Many paths to synaptic specificity. *Annu Rev Cell Dev Biol* 25:161–195.
4. ten Donkelaar HJ, et al. (2004) Development and malformations of the human pyramidal tract. *J Neurol* 251:1429–1442.
5. Martin JH (2005) The corticospinal system: From development to motor control. *Neuroscientist* 11:161–173.
6. Lemon RN (2008) Descending pathways in motor control. *Annu Rev Neurosci* 31:195–218.
7. Rathelot JA, Strick PL (2009) Subdivisions of primary motor cortex based on cortico-motoneuronal cells. *Proc Natl Acad Sci USA* 106:918–923.
8. O'Leary DD, Koester SE (1993) Development of projection neuron types, axon pathways, and patterned connections of the mammalian cortex. *Neuron* 10:991–1006.
9. McConnell SK (1995) Constructing the cerebral cortex: Neurogenesis and fate determination. *Neuron* 15:761–768.
10. Rash BG, Grove EA (2006) Area and layer patterning in the developing cerebral cortex. *Curr Opin Neurobiol* 16:25–34.
11. Molyneaux BJ, Arlotta P, Menezes JR, Macklis JD (2007) Neuronal subtype specification in the cerebral cortex. *Nat Rev Neurosci* 8:427–437.
12. Molyneaux BJ, Arlotta P, Hirata T, Hibi M, Macklis JD (2005) *Fezl* is required for the birth and specification of corticospinal motor neurons. *Neuron* 47:817–831.
13. Chen JG, Rasin MR, Kwan KY, Sestan N (2005) Zfp312 is required for subcortical axonal projections and dendritic morphology of deep-layer pyramidal neurons of the cerebral cortex. *Proc Natl Acad Sci USA* 102:17792–17797.
14. Chen B, Schaevitz LR, McConnell SK (2005) *Fezl* regulates the differentiation and axon targeting of layer 5 subcortical projection neurons in cerebral cortex. *Proc Natl Acad Sci USA* 102:17184–17189.
15. Kwan KY, et al. (2008) SOX5 postmitotically regulates migration, postmigratory differentiation, and projections of subplate and deep-layer neocortical neurons. *Proc Natl Acad Sci USA* 105:16021–16026.
16. Lai T, et al. (2008) SOX5 controls the sequential generation of distinct corticofugal neuron subtypes. *Neuron* 57:232–247.
17. Bedogni F, et al. (2010) Tbr1 regulates regional and laminar identity of postmitotic neurons in developing neocortex. *Proc Natl Acad Sci USA* 107:13129–13134.
18. Hevner RF, et al. (2001) Tbr1 regulates differentiation of the preplate and layer 6. *Neuron* 29:353–366.
19. Kispert A, Hermann BG (1993) The *Brachyury* gene encodes a novel DNA binding protein. *EMBO J* 12:4898–4899.
20. Wang TF, et al. (2004) Identification of Tbr-1/CASK complex target genes in neurons. *J Neurochem* 91:1483–1492.
21. Jacobs EC, et al. (2007) Visualization of corticofugal projections during early cortical development in a τ-GFP-transgenic mouse. *Eur J Neurosci* 25:17–30.
22. Bulfone A, et al. (1998) An olfactory sensory map develops in the absence of normal projection neurons or GABAergic interneurons. *Neuron* 21:1273–1282.
23. Iwasato T, et al. (2004) Dorsal telencephalon-specific expression of Cre recombinase in PAC transgenic mice. *Genesis* 38:130–138.
24. Kawamoto S, et al. (2000) A novel reporter mouse strain that expresses enhanced green fluorescent protein upon Cre-mediated recombination. *FEBS Lett* 470:263–268.
25. Catsman-Berrevoets CE, Kuypers HGJM (1981) A search for corticospinal collaterals to thalamus and mesencephalon by means of multiple retrograde fluorescent tracers in cat and rat. *Brain Res* 218:15–33.
26. Johnson MB, et al. (2009) Functional and evolutionary insights into human brain development through global transcriptome analysis. *Neuron* 62:494–509.
27. Donoghue MJ, Rakic P (1999) Molecular evidence for the early specification of presumptive functional domains in the embryonic primate cerebral cortex. *J Neurosci* 19:5967–5979.
28. Gong S, et al. (2003) A gene expression atlas of the central nervous system based on bacterial artificial chromosomes. *Nature* 425:917–925.
29. McKenna WL, et al. (2011) *Tbr1* and *Fezf2* regulate alternate corticofugal neuronal identities during neocortical development. *J Neurosci* 31:549–564.

Supporting Information

Han et al. 10.1073/pnas.1016723108

SI Materials and Methods

Immunostaining. Brains dissected from embryonic and neonatal animals were fixed by immersion in 4% paraformadehyde overnight at 4 °C. Adult brains were fixed by perfusion, dissected, and post-fixed by immersion in 4% paraformadehyde overnight at 4 °C. Brains were vibratome-sectioned at 70 μm (Leica VT1000S). The sections were blocked and immunostained. The following primary antibodies were used at the indicated dilution: anti-CldU (rat, 1:100; Accurate Chemical), anti-GFP (chicken, 1:3,000; Abcam), anti-SOX5 (rabbit, 1:100; Genway), anti-TBR1 (rabbit, 1:250; Abcam and Santa Cruz Biotechnology), anti-ZFPM2 (rabbit, 1:250; Santa Cruz Biotechnology), anti-RFP (rabbit, 1:1,000; US Biological), anti-IdU (mouse, 1:200; BD Biosciences), anti-CUX1 (rabbit, 1:150; Santa Cruz Biotechnology), anti-SATB2 (mouse, 1:200; Santa Cruz Biotechnology), anti-NF1B (rabbit, 1:300; Active Motif), and anti-BC11B (rat, 1:250; Santa Cruz Biotechnology).

Plasmid Constructs. For TBR1 expression, full-length mouse *Tbr1* cDNA (BC052737) was inserted into pCAGEN (1). For ChIP, a N-terminal V5 tag (GKPIPNPLLGLDST) was added to create the pCAG-V5-*Tbr1* construct. Luciferase reporter plasmids were made by inserting annealed 57-bp-long complementary oligos representing the TBR1 biding site near *Fezf2* into the SalI site of pGL3-CMV plasmid. pGL3-CMV was made by replacing the SV40 promoter of pGL3-promoter plasmid (Promega) with a CMV promoter.

Layer Distribution Analysis. To quantify the distribution of neurons, the P0–P14 neocortex was divided radially into 10 equal-sized bins from the pia to the upper edge of the white matter. For E15.5 analyses, the pia to the upper edge of the intermediate zone was divided radially into six bins. The cells in each bin were quantified and reported as the percentage of total cells counted.

Thymidine Analog Labeling. Timed-pregnant mice were injected intraperitoneally with 40 mg/kg body weight of CldU. Brain sections were subjected to acidic antigen retrieval before blocking.

Retrograde Axonal Tracing. For in vivo retrograde tracing, rhodamine-conjugated LMS (Lumafluor) were injected into the target region of neonatal or P3 live mice under ice anesthesia. The brains of injected neonatal mice were dissected after survival for 18–24 h and fixed. The injected P3 mice were fixed by perfusion at P7. The injection site of all injected brains was verified both externally and in sections through the injection site. Only brains that were clearly and specifically injected at the correct location were used. Quantitative analyses of retrogradely labeled neurons were consistently performed in the same area in the somatosensory cortex to allow direct comparisons of brains. Confocal images with an optical thickness of 2 μm were used for all quantifications. A square box encompassing the entire cortical plate from the upper edge of the white matter to the upper edge of the marginal zone was overlaid, and all neurons within the box were quantified.

Luciferase Assays. N2A cells were plated and transfected with firefly luciferase (pGL3-CMV) containing a TBR1 binding site as described previously (2). Transfected cells were lysed and assayed 24 h later using a Promega Luciferase Reporter Kit. qRT-PCR of pGL3-CMV was performed to normalize for transfection efficiency.

mRNA-Seq and Data Analysis. Total RNA was isolated from freshly dissected P0 neocortices of $Tbr1^{-/-}$ and $Tbr1^{+/+}$ littermates using a Qiagen RNeasy Mini Kit. Libraries were prepared using an Illumina mRNA-Seq Sample Prep Kit. Amplified cDNA was size-selected at 250 bp and validated using the Agilent Bioanalyzer DNA 1000 system. The final product was subjected to cluster generation using an Illumina Standard Cluster Generation Kit v4. Libraries were sequenced as single end 74mers using the Illumina Genome Analyzer pipeline, and image analysis (Firecrest module), base-calling (Bustard module), and primary sequence analysis (Gerald module) were performed. Reads were mapped to the mouse reference genome (release mm9) with ELAND software. Filtered reads that were uniquely mapped to exons of Ensembl gene model with up to two mismatches were used for the quantification of gene expression. To detect differentially expressed genes between $Tbr1^{-/-}$ and $Tbr1^{+/+}$, we designed a three-step stringent filtering process. First, counts of mapped reads within genes were compared using Fisher's exact test (adjusted $P \leq 0.05$). Second, reads per kb of exon model per million reads (RPKM = $10^9 C/NL$, where C is the number of mappable reads that fall onto the gene's exons, N is the total number of mappable reads in the lane, and L is the sum of the exons in base pairs) were used to quantify gene expression, and the fold change was set as another filtering scale ($|\log2(\text{fold change})| \geq 0.5$) (3). In our series of relative experiments, the genes were finally identified as differentially expressed unless they were shared by all groups.

mRNA Sequencing Uniformity. One gene with n exons was assigned as one vector, G = {R1,R2,. . .,Ri,. . .,Rn}, where Ri is the ratio of the ith exon expression (in RPKM) relative to the mean expression of n exons. The Ri values were sorted according to the exon order from 5′ to 3′. Isoforms were combined to obtain the longest gene. Because different genes generally had different values of n, they were zoomed into the same length by uniformly filling some gaps in genes with fewer exons (e.g., G = {R1,GAP, R2,. . .,GAP,Ri,. . .,GAP,Rn}). The uniformity of the G vector from 5′ to 3′, quantified by mean and standard variation, directly reflected the degree of mRNA sequencing uniformity.

ChIP-Seq and Data Analysis. ***Cell Preparation.*** N2A cells were transfected with pCAG-V5-*Tbr1* plasmid using Lipofectamine 2000 (Invitrogen). At 48 h after transfection, cells were harvested using a silicon scraper, transferred to a 50-mL conical tube, crosslinked by adding 1/10 volume of crosslinking solution for 15 min, and quenched by adding 1/10 volume of a 1.25 M glycine solution. Crosslinked cells were washed, flash-frozen in liquid nitrogen, and stored at −80 °C.

ChIP. ChIP was performed following a protocol modified from Lee et al. (4). Crosslinked cells were thawed on ice and lysed. Lysates were sonicated (with a Misonix 4000) to shear the chromatin to 200∼500 bp for ChIP-Seq. For each ChIP reaction, 1000 μg of sheared chromatin was incubated overnight at 4 °C with Dynal Protein A/G beads bound to anti-V5 antibody (rabbit, 1:10; Abcam) to precipitate V5-TBR1. Dynabeads were washed extensively and then eluted at 65 °C for 15 min with occasional vortexing. Eluted protein–chromatin complexes were reverse-crosslinked by overnight incubation at 65 °C. ChIPed and input DNA were treated with RnaseA and proteinase K and then purified.

Library Preparation and Sequencing. An Illumina ChIP-Seq library preparation kit was used in accordance with the manufacturer's instructions with modifications. DNA fragments were end-

repaired, "A" bases were added to the 3′ end, and sequencing adaptors were ligated. To reduce the free adaptor dimers that could be preferentially amplified during PCR, the amount of adaptors added was reduced to 1:30 or 1:40 instead of 1:10. After ligation, PCR amplification was performed first, and 250- to 350-bp fragments were size-selected. Gel extraction was performed at room temperature to avoid the decreased representation of an A+T-rich sequence. Libraries were sequenced with an Illumina GAII Sequencing System in accordance with the manufacturer's protocol.

Data Analysis. All 36-bp reads were aligned to the mouse reference genome (NCBI build 37, mm9) using the bowtie program. Only uniquely aligned reads were used for subsequent analysis. The numbers of reads that fell into each 50-bp shift window were calculated across whole chromosomes. A single bedGraph data file was created for each reaction and uploaded to the UCSC Genome Browser (http://genome.ucsc.edu/).

Determination of TBR1 Consensus Binding Sequence. All 36-bp reads from V5 antibody ChIP were aligned to the mouse genome mm9 as described above. All reads for input were aligned as well. Then a sliding-window approach, with a window size of 200 bp and a shift step of 50 bp, was used to detect enriched genome regions. Windows enriched in the V5 experiment by 20-fold greater than expected were selected. Overlapping enriched windows were merged into one enriched region. To minimize background signals, regions enriched in the control experiment by fivefold greater than expected were removed from the enriched list. A proximal gene with minimum distance was selected for each enriched region. Genomic information of all genes was downloaded from the UCSC Genome Browser.

To specifically select for sites to which TRB1 binding led to changes in gene expression, only genes that were proximal to enriched regions were chosen for determination of the consensus binding sequence. Only genes with differential expression between *Tbr1*$^{+/+}$1 and *Tbr1*$^{-/-}$1 and also between *Tbr1*$^{+/+}$2 and *Tbr1*$^{-/-}$2 were selected for the final list of candidate genes regulated by *Tbr1*. All enriched regions whose proximal genes were in the foregoing candidate list were selected. The PRIORITY program (http://www.cs.duke.edu/~amink/software/priority/) was used to search for consensus sequences, with the following parameters: a motif length of 20, a flat prior, a third-order background model, 50 trials, and 10,000 iterations per trial. For the TBR1 binding site, the multispecies conservation analysis was performed using the 30-way Multiz Alignment and Conservation track in the UCSC Genome Browser.

ChIP qRT-PCR. ***Cell Preparation.*** Primary cortical neurons were prepared from microdissected E13.5 *Fezf2-Gfp* transgenic cortices and transfected with pCAG-V5-*Tbr1* plasmid DNA using the amaxa Mouse Neuron Nucleofector Kit (VPG-1001; Lonza). At 48 h after transfection, cells were collected as described above.

ChIP. Primary neuronal lysates were sonicated to shear the chromatin to 200-1,000 bp for ChIP–qRT-PCR. ChIP was performed as described above for ChIP-Seq.

qRT-PCR of ChIPed DNA. For the qRT-PCR reactions, 500 pg of ChIP sample was amplified using SYBR green PCR Master Mix (Roche). Thermocycling was carried out using the Applied Biosystems 7900 System. Input DNA values were used for normalization.

Nuclear Size Analysis. Coronal sections from LMS-traced *Tbr1*$^{+/+}$*; Golli-Gfp* and *Tbr1*$^{-/-}$*;Golli-Gfp* littermate brains (n = 2 for each genotype) were immunostained for GFP and ZFPM2 and nuclear-stained using DAPI. WT L5 CS neurons (LMS^{+}), WT L6 neurons (*Golli-Gfp*$^{+}$ and ZFPM2^{+}), and *Tbr1*$^{-/-}$ L6 CS neurons (LMS^{+}, *Golli-Gfp*$^{+}$, and ZFPM2^{+}), were examined by confocal microscopy (n = 30 cells per cell type). The plane of focus was adjusted precisely so that the nucleus of the cell of interest was at its roundest and largest. The length of the longest diameter drawn on the nucleus was used for analysis.

Generation of Fezf2 Conditional Knockout Mice. The targeting vector for conditional inactivation of *Fezf2* was constructed by a recombineering-based method (5) with a bacterial artificial chromosome (BAC; clone RP23-141E17). Exon 2, which encodes amino acids 1–279 of 455, was targeted for removal. An 11-kb fragment containing exon 2 was retrieved from the BAC clone and inserted into the PL253 vector by recombination in the bacterial strain SW102. PGK-neo was used as a positive selection marker, and the MC1-TK (thymidine kinase) cassette was used as a negative selection marker. The loxP/Frt-flanked positive selectable marker and the loxP site for conditional deletion of exon 2 were inserted as described in Fig. 8*A*. The linearized targeting construct was electroporated into embryonic stem cells, which were then subjected to G418 selection. Clones positive for homologous recombination were identified by long-distance PCR and confirmed by sequencing before blastocyst injection. Cortex-specific deletion of exon 2 was achieved using the *Emx1-Cre* PAC transgene.

qRT-PCR. Total RNA isolated for mRNA-Seq was also used for qRT-PCR. Template cDNA was synthesized, and predesigned primer and probe sets were used.

1. Matsuda T, Cepko CL (2007) Controlled expression of transgenes introduced by in vivo electroporation. *Proc Natl Acad Sci USA* 104:1027–1032.
2. Abelson JF, et al. (2005) Sequence variants in *SLITRK1* are associated with Tourette's syndrome. *Science* 310:317–320.
3. Mortazavi A, Williams BA, McCue K, Schaeffer L, Wold B (2008) Mapping and quantifying mammalian transcriptomes by RNA-Seq. *Nat Methods* 5:621–628.
4. Lee TI, et al. (2006) Control of developmental regulators by Polycomb in human embryonic stem cells. *Cell* 125:301–313.
5. Liu P, Jenkins NA, Copeland NG (2003) A highly efficient recombineering-based method for generating conditional knockout mutations. *Genome Res* 13:476–484.
6. Kispert A, Hermann BG (1993) The *Brachyury* gene encodes a novel DNA binding protein. *EMBO J* 12:4898–4899.
7. Hevner RF, et al. (2001) Tbr1 regulates differentiation of the preplate and layer 6. *Neuron* 29:353–366.
8. Chen B, Schaevitz LR, McConnell SK (2005) *Fezl* regulates the differentiation and axon targeting of layer 5 subcortical projection neurons in cerebral cortex. *Proc Natl Acad Sci USA* 102:17184–17189.
9. Molyneaux BJ, Arlotta P, Hirata T, Hibi M, Macklis JD (2005) *Fezl* is required for the birth and specification of corticospinal motor neurons. *Neuron* 47:817–831.

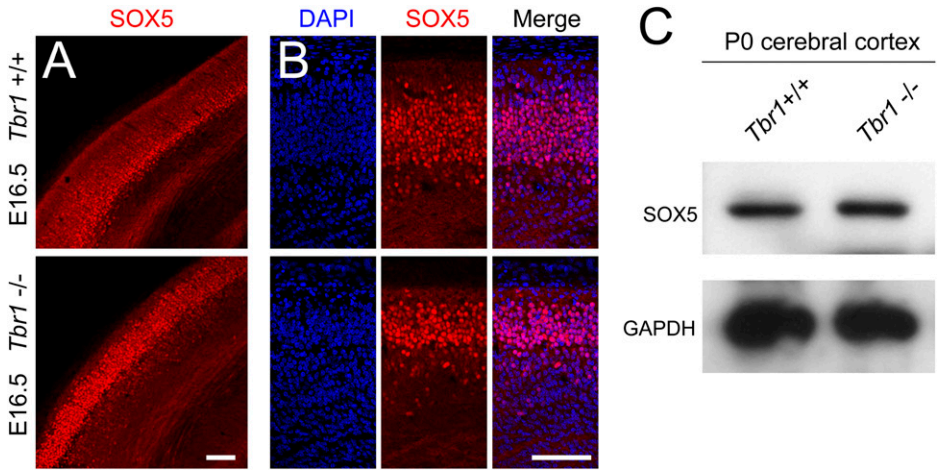

Fig. S1. SOX5 protein levels were largely unaltered in the late embryonic and neonatal *Tbr1*$^{-/-}$ neocortex. (*A* and *B*) Immunofluorescent staining for SOX5 at E16.5 revealed intense nuclei staining in the cortical plate of *Tbr1*$^{-/-}$, comparable to that seen in *Tbr1*$^{+/+}$ embryos. (*C*) Neocortical lysates were collected from *Tbr1*$^{-/-}$ and *Tbr1*$^{+/+}$ P0 littermates. Western blot analysis revealed that SOX5 protein levels were not significantly altered in *Tbr1*$^{-/-}$ at P0. GAPDH was used as a loading control. (Scale bars: 100 μm.)

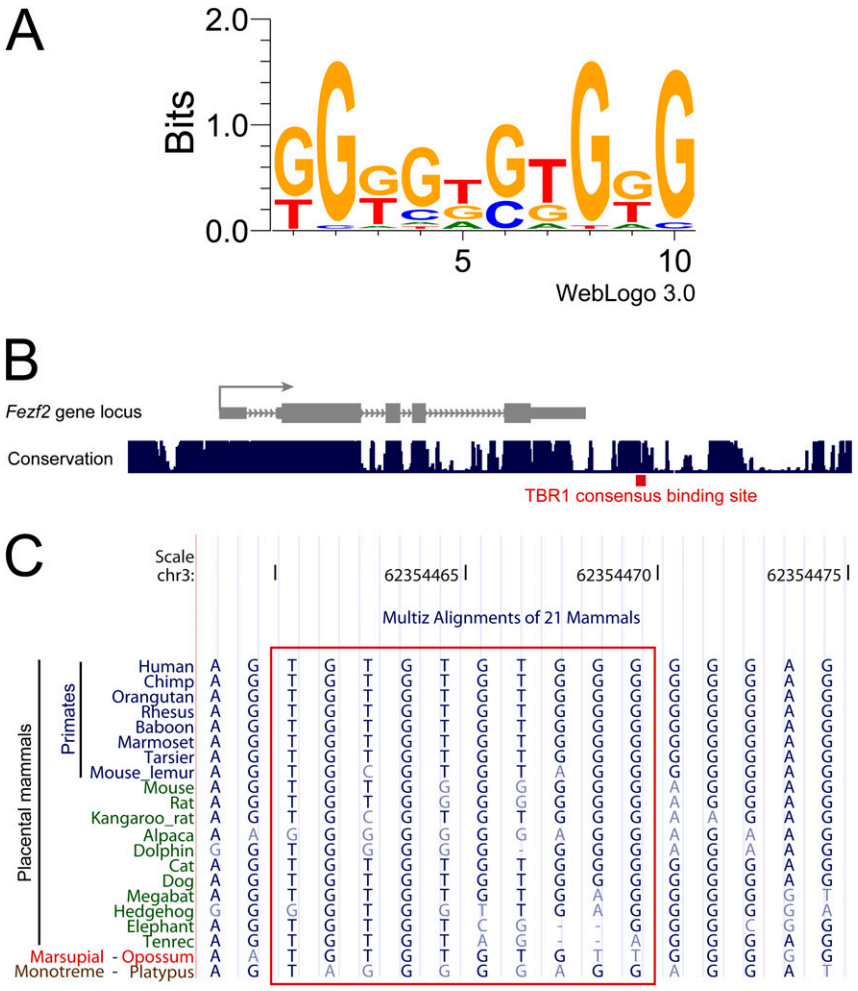

Fig. S2. Direct TBR1 binding of a novel 10-bp consensus binding site near *Fezf2* was defined by global analysis of ChIP-Seq reads. (*A*) A computational screen for an enriched consensus motif with nucleotide bias using Weblogo 3. This novel TBR1 binding sequence motif is similar to the reported TBR1 binding site in *Xenopus* determined using random oligonucleotides (6). (*B*) A region 4.5 kb downstream of the *Fezf2* TSS with significant enrichment of V5-TBR1 ChIP-Seq reads over input DNA. This region contains a consensus TBR1 binding sequence motif (red). (*C*) Sequence alignment of the TBR1 binding motif (red box) across 21 mammalian species demonstrating high conservation.

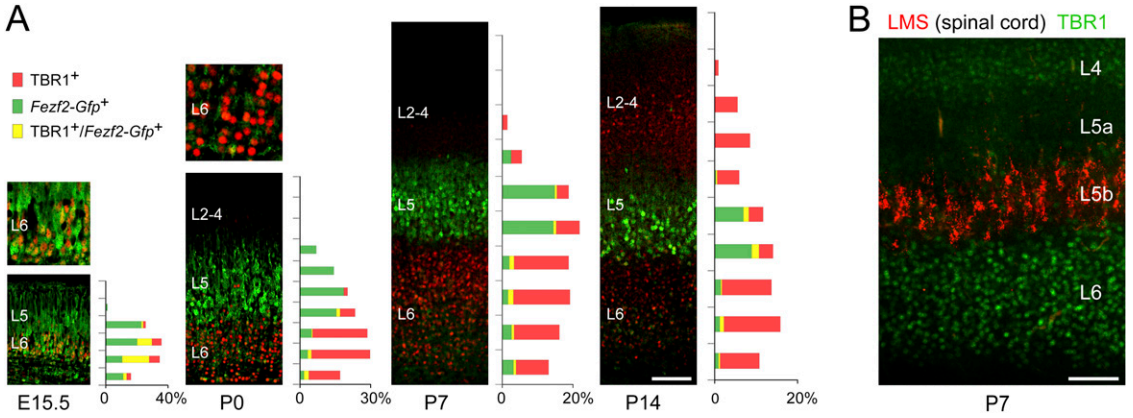

Fig. S3. TBR1 was expressed in a pattern highly complementary to *Fezf2* and was excluded from CS neurons in early postnatal neocortex. (*A*) Neocortices of *Fezf2-Gfp* (green) transgenic mice were immunostained for TBR1 (red). At E15.5, before the onset of postmigratory down-regulation of *Fezf2* in L6, 63.5% of TBR1$^+$ L6 neurons coexpressed high levels of *Fezf2-Gfp* (yellow). At P0, *Fezf2-Gfp* was highly expressed in L5 neurons but was down-regulated in L6 and SP neurons, which expressed TBR1 abundantly. Only 7.7% of TBR1$^+$ neurons coexpressed *Fezf2-Gfp* at this stage. This almost mutually exclusive pattern of gene expression in L5 and L6 was maintained into the early postnatal stages. Starting at P7, TBR1 was also expressed at low levels in L2–L4, in which *Fezf-Gfp* was completely absent. (*B*) The retrograde tracer LMS (red) was injected into the cervical spinal cord of live mice at P3, and the mice were killed at P7. All retrogradely traced CS neurons were positioned in L5b; none expressed detectable TBR1 (green). This absolute exclusion of TBR1 from early postnatal CS neurons and its highly complementary expression with *Fezf2* suggest that TBR1 is a compelling candidate for putatively restricting high *Fezf2* expression to L5 neurons. (Scale bars: 100 μm.)

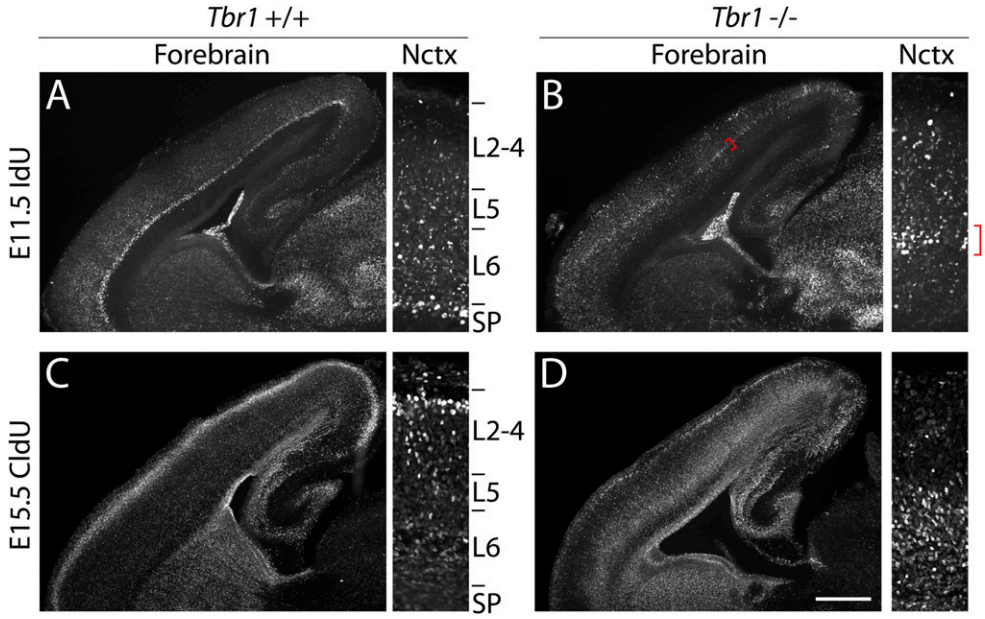

Fig. S4. Thymidine analog birth-dating confirmed migration defects and revealed an ectopic band of cells containing early-born neurons in *Tbr1*$^{-/-}$ neocortex (Nctx). (*A* and *B*) IdU was injected into timed-pregnant females at E11.5, when SP and L6 neurons are generated. (*A*) At P0, neurons born at E11.5 were positioned in the SP and the lower portion of L6 in the *Tbr1*$^{+/+}$. (*B*) In P0 *Tbr1*$^{-/-}$, neurons born at E11.5 were positioned primarily in a thin ectopic band of cells (red brackets) located in the middle of the cortical plate, indicating defects in neuronal migration and preplate segregation. In addition to this band of cells, a considerable proportion of early-born neurons were dispersed to all cortical layers. (*C* and *D*) CldU was injected into timed-pregnant females at E15.5, when upper layer neurons are born. In P0 *Tbr1*$^{+/+}$, these late-born neurons migrated to L2–L3 (*C*). In P0 *Tbr1*$^{-/-}$, most of these late-born neurons were ectopically positioned at deep levels of the neocortex (*D*). Although their distribution was more dispersed, a small proportion of E15.5-labeled neurons migrated to L2. (Scale bar: 500 μm.)

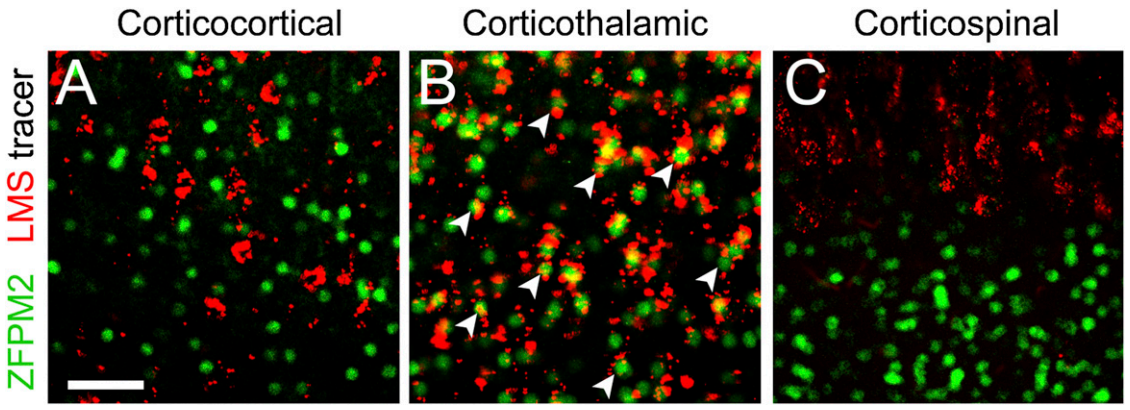

Fig. S5. ZFPM2 (also known as FOG2) is a highly specific marker of corticothalamic projection neurons. Neurons of distinct projectional subclasses in P7 WT neocortex were retrogradely labeled using the tracer LMS (red). LMS was injected into the contralateral neocortex, ipsilateral dorsal thalamus, or cervical spinal cord at P3 to label corticocortical, corticothalamic, or CS neurons, respectively. Coronal sections from traced brains were immunostained for ZFPM2 (green). None of the retrogradely labeled corticocortical or CS neurons was positive for ZFPM2 (*A* and *C*). In contrast, virtually all neurons labeled by LMS injected into the dorsal thalamus were ZFPM2^{+} (*B*, solid arrowheads), indicating that ZFPM2 is a highly specific marker of corticothalamic projection neurons. (Scale bar: 50 μm.)

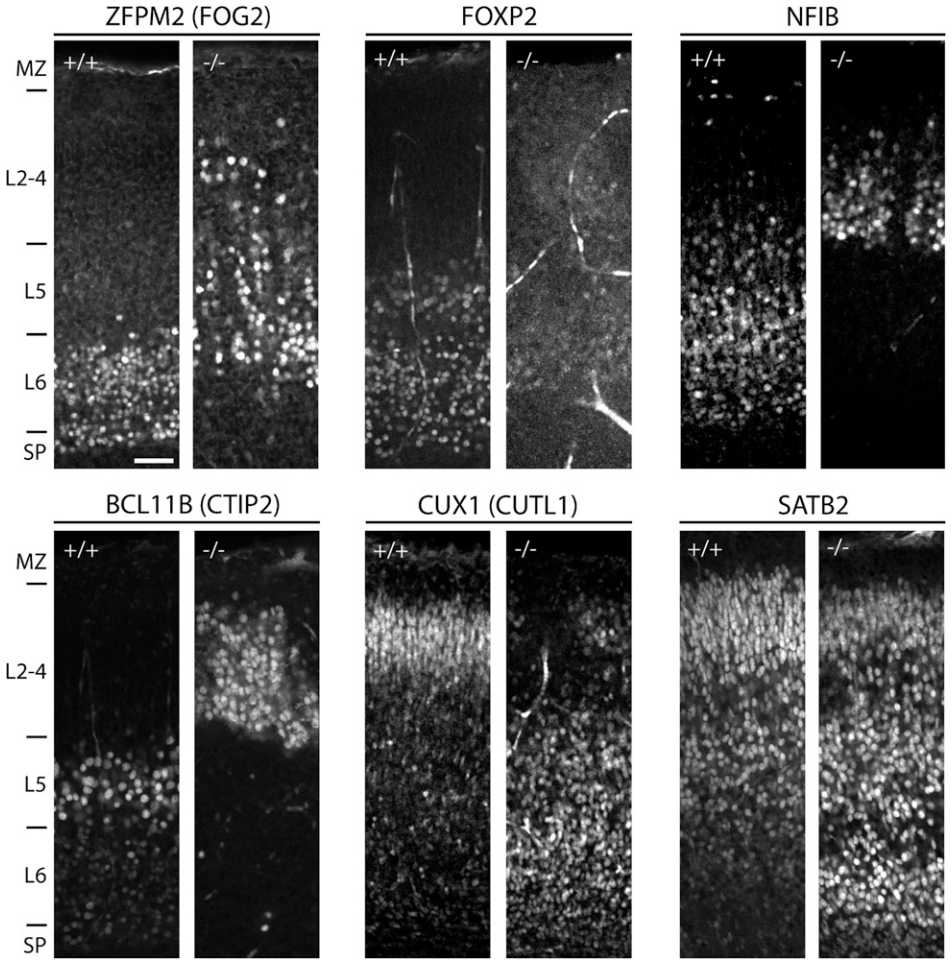

Fig. S6. Expression of layer-specific markers in *Tbr1*$^{-/-}$ neocortex. P0 neocortices were immunostained with the indicated primary antibodies. In *Tbr1*$^{-/-}$ neocortex, most deep-layer neurons were positioned within clusters, as described previously (7). The molecular markers of L6 neurons were differentially affected. Expression of the L6 markers FOXP2 and NFIB was diminished, whereas that of ZFPM2 was normal. Expression of the L5 marker BCL11B was slightly increased. Most upper-layer neurons of the *Tbr1*$^{-/-}$ neocortex (denoted by CUX1 and SATB2) did not migrate to their normal destination; instead, they were dispersed, mostly located in the deeper portion of the neocortex and largely absent from the clusters containing L5 and L6 neurons. The expression levels of CUX1 and SATB2 were not diminished, however. (Scale bar: 50 μm.)

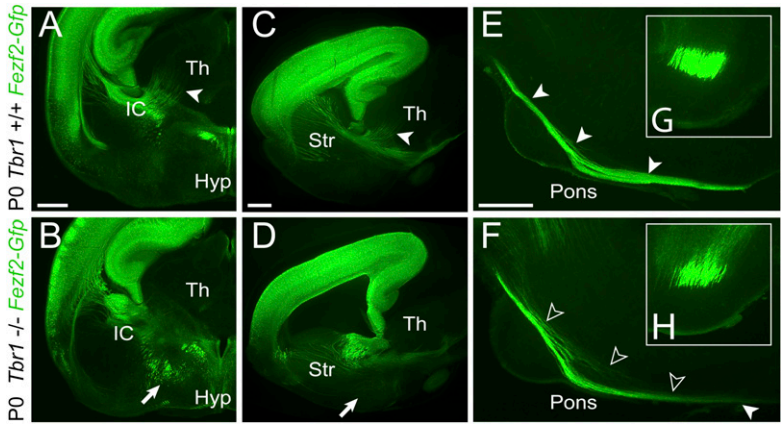

Fig. S7. Specific defects in *Tbr1*$^{-/-}$ subcortical axon tracts. P0 coronal (*A*) and sagittal (*B* and *C*) sections of *Tbr1*$^{-/-}$ and *Tbr1*$^{+/+}$ littermates transgenic for *Fezf2-Gfp*. (*A–D*) In the *Tbr1*$^{+/+}$ brain, *Fezf2-Gfp*$^{+}$ axons abundantly innervated the thalamus (solid arrowheads). In the *Tbr1*$^{-/-}$ brain, no *Fezf2-Gfp*$^{+}$ axons innervated the dorsal thalamus, indicating complete loss of the corticothalamic tract. Ectopic subcortical axons innervated the basal forebrain (arrows), and the stereotypical organization of the internal capsule was lost. (*E* and *F*) The CS tract of the *Tbr1*$^{-/-}$ (open arrowheads) was similar to that of the *Tbr1*$^{+/+}$ (solid arrowheads). Some of the *Tbr1*$^{-/-}$ CS axons were less tightly bundled and followed a more dorsal trajectory through the ventral pons. (*G* and *H*) The thickness of the CS tract was unaffected in *Tbr1*$^{-/-}$, indicating that the number of CS axons was not significantly altered. (Scale bars: 500 μm.)

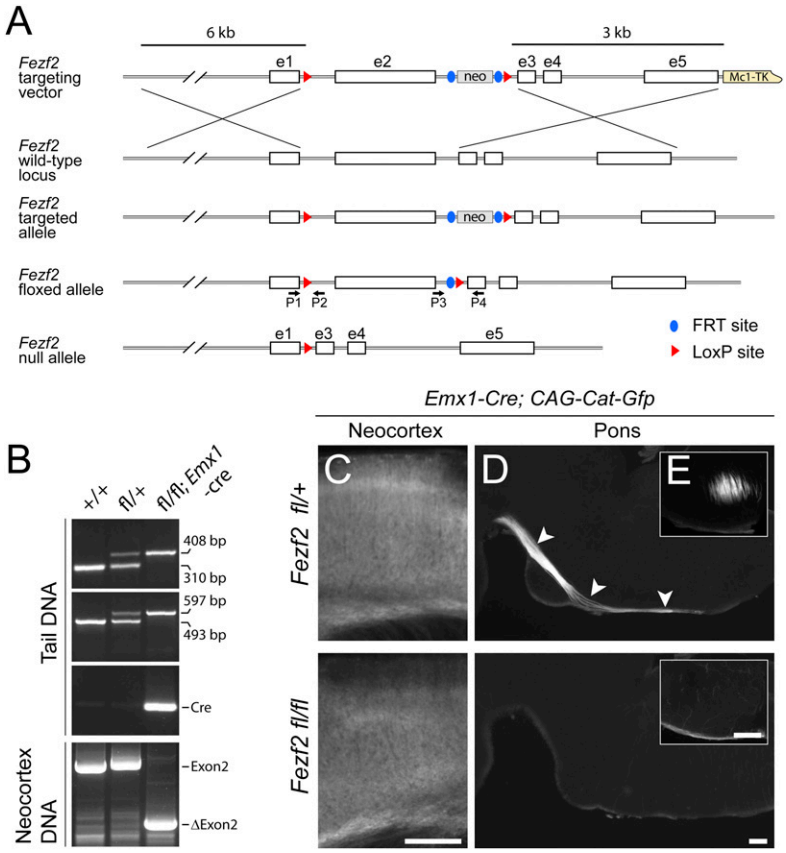

Fig. S8. Cortex-specific conditional deletion of *Fezf2* phenocopies germ-line *Fezf2* null mutation. (*A*) Schematic of the targeting strategy used for generating a floxed *Fezf2* allele. Cortex-specific deletion of *Fezf2* was achieved using the *Emx1-Cre* transgene. (*B*) Correct insertion of loxP sites and presence of the *Emx1-Cre* transgene were confirmed by PCR of genomic DNA extracted from tail biopsy specimens. CRE-mediated recombination exon 2 in the cortex was confirmed by PCR of DNA extracted from neocortices of *Fezf2*$^{flox/flox}$*;Emx1-Cre* mice. (*C–E*) To examine the pancortical pattern of axonal connectivity, *Fezf2*$^{flox/flox}$*;Emx1-Cre* mice were further crossed with *CAG-Cat-Gfp* transgenic mice. CRE-mediated recombination occurred in all neocortical projection neurons and activated GFP expression from the *CAG-Cat-Gfp* transgene (*C*). Analysis of GFP-filled axons of cortical projection neurons revealed that the CS tract was completely absent (*D* and *E*), phenocopying germ-line knockouts of *Fezf2* (8, 9). (Scale bars: 200 μm.)

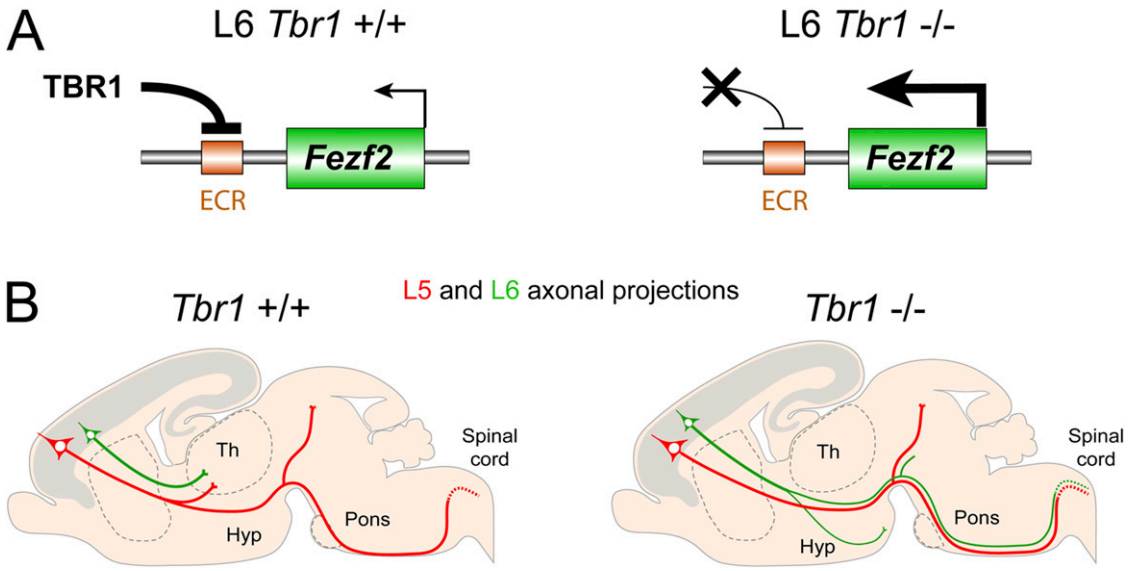

Fig. S9. Schematic summary of *Tbr1*$^{-/-}$ defects in regulation of *Fezf2* transcription (*A*) and the laminar origin of distinct subcortical projection subtypes (*B*). In L6 neurons of the *Tbr1*$^{+/+}$ neocortex, TBR1 binds to an evolutionarily conserved consensus motif near the *Fezf2* locus and represses the expression of *Fezf2*. In *Tbr1*$^{-/-}$ neocortices, L6 neurons aberrantly turn on high *Fezf2* expression. Concomitant with increased *Fezf2* expression, *Tbr1*$^{-/-}$ L6 neurons project ectopically to the hypothalamus (Hyp) and brainstem.